Earth Planets Space, **64**, 577–593, 2012

Equatorial vertical plasma drifts and the measured and IRI model-predicted F_2-layer parameters above Ouagadougou during solar minimum

O. S. Oyekola

307-143 Eighth Street, Etobicoke, Ontario, Canada M8V 3C8

(Received July 27, 2011; Revised October 16, 2011; Accepted October 20, 2011; Online published July 27, 2012)

In this paper, hourly median value of ionosonde measurements: peak height F_2-layer (h_mF_2), F_2-layer critical frequency (f_oF_2) and propagation factor $M(3000)F_2$ made at near-equatorial dip latitude, Ouagadougou, Burkina Faso (12°N, 1.5°W; dip: 1.5°N) and relevant F_2-layer parameters: thickness parameter (B_o), electron temperature (T_e), ion temperature (T_i), total electron content (TEC) and electron density (N_e) (at the fixed altitude of 300 km) provided by the International Reference Ionosphere (IRI) model for the longitude of Ouagadougou are contrasted with the IRI vertical drift model to explore in detail the monthly climatological behavior of equatorial ionosphere and the effects of equatorial electrodynamics on the diurnal structure of F_2-layer parameters. The analysis period covers four months representative of solstitial and equinoctial seasonal periods during solar minimum year of 1987 for geomagnetically quiet-day. It is demonstrated that the month-by-month morphological patterns between vertical $\mathbf{E} \times \mathbf{B}$ drifts and F_2-layer parameters range from worst to reasonably good and are largely seasonally dependent. A cross-correlation analysis conducted between equatorial drift and F_2-layer characteristics yield statistically significant correlations for equatorial vertical drift and IRI-B_o, IRI-T_e and IRI-TEC, whereas little or no acceptable correlation is obtained with observational evidence. Examination of the association between measured f_oF_2, h_mF_2 and $M(3000)F_2$ illustrates consistent much more smaller correlation coefficients with no systematic linkage.

Key words: Equatorial-ionosphere, vertical-drift, ionospheric-parameter, correlation-analysis, solar-minimum, IRI.

1. Introduction

Equatorial vertical plasma drift is an important consequence of the E and F region dynamos (Alken, 2009). Equatorial zonal electric fields control the vertical plasma transport in the low-latitude ionosphere (Kelley, 1989; Fejer, 1997). It drives the equatorial electrojet and the equatorial ionization anomalies (Rush and Richmond, 1973; Kelley, 1989). In the evening hours, it drives plasma to higher heights increasing the linear instability growth rate of spread F plasma instabilities (Kelley, 1989; Sultan, 1996). Fejer *et al*. (1991) discussed extensively the large day-to-day variability in vertical drift velocities as determined by Jicamarca Incoherent Scatter Radar (JISR), located at the magnetic equator in Peru in the West Coast of South American. Scherliess and Fejer (1999) presented the first comprehensive study of global empirical model of the quiet-time F region equatorial vertical drifts based on combined incoherent scatter radar (ISR) observations at Jicamarca and ion drift meter (IDM) measurements on board the Atmospheric Explorer E (AE-E) satellite. Their study presents local time, season, solar cycle and longitude effects on quiet-time equatorial F region vertical plasma drifts. The physical principles underlying the electrodynamic properties of the equatorial and mid-latitude ionosphere is discussed in a tutorial given by Heelis (2004).

Observations of vertical plasma drifts in the equatorial region of the African ionosphere have also been inferred from ionosonde observations mostly during nighttime solar maximum magnetospherically quiet conditions (e.g., Oyekola *et al*., 2007, 2008; Oyekola and Oluwafemi, 2007, 2008; Oyekola, 2009a, b; Oyekola and Kolawole, 2010). By and large, except for magnitude the characteristic features of equatorial electromagnetic drifts in the African ionosphere are in good agreement with those obtained for the equatorial region in the America sector using ISR observations (e.g., Fejer *et al*., 1979, 1991). The general diurnal features are as follows: The F region electrodynamic plasma drifts are upward and westward during the day and downward and eastward at night. The daytime drifts have largest amplitudes between about 0900 and 1100 LT with typical values of 25–30 m/s. The drift exhibits morning and evening reversals from downward nighttime to upward daytime and from upward daytime to downward nighttime, respectively. The morning reversal times and the daytime drifts indicate just little variations with the phase of the solar cycle. Around dusk hours, there is an enhancement in the vertical drift of the F layer plasma, which is produced by an enhancement in the zonal electric field, known as the evening prereversal electric field enhancement (PRE). In particular, during solar minimum the prominent feature of equatorial ionosphere, the evening prereversal velocity enhancement re-

doi:10.5047/eps.2011.10.008

veals small longitudinal changes with largest usually occur in equinoxes, intermediate value in December solstice, and absent at all longitudes during June solstice season.

The International Reference Ionosphere (IRI) is a global empirical model, which describes the average behavior of ionospheric electron density (N_e) at 300 km height, electron and ion temperatures (T_e and T_i), equatorial $\mathbf{E} \times \mathbf{B}$ drift velocity (V_z), total electron content (TEC) and ion composition (Bilitza, 1990, 2001, 2003; Bilitza *et al*., 2004a, and references therein). As an empirical model based on mixed data, the IRI is obviously only as good as the available observations. The data sources used in the IRI model comprise mid-latitude ionosonde, ISR, rocket as well as satellite measurements. Moreover, the IRI is a six-segment model (Bilitza, 2001, 2003) covering height ranges from D region to the topside. For an update on the considerable progress of IRI-prediction model see Bilitza and Reinisch (2008).

The ionospheric F_2-layer parameters are used to typify the quiet-day climatological behavior of the ionosphere for different levels of solar activity. The peak parameters such as f_oF_2, h_mF_2 (or $M_{3000}F_2$ to which as a first order it is inversely correlated) are valuable in generating representative plasma density height profiles appropriate to particular probabilities of occurrence, while the thickness and shape parameters (B_o, B_1) are used to characterize the bottomside of F_2-layer electron concentration altitude profiles (Bradley *et al*., 2004). The parameters N_mF_2, h_mF_2, B_o, and B_1 are related to the plasma density altitude profiles, $N_e(h)$ by the analytic expression given by Bilitza (1990):

$$N_e(h) \equiv N_mF_2 * \frac{\exp\left(-x^{B_1}\right)}{\cosh(x)}, \tag{1}$$

with

$$x = \frac{h_mF_2 - h}{B_o},$$

where h is the altitude. On the other hand, total electron content (TEC) is a parameter of great importance for the phase delay of high-frequency ground-to-satellite signals. Electron and ion temperatures (T_e and T_i), on the other hand, carry major information on the thermal properties in the ionosphere.

However, a number of prior publications have pursued the correlations between individual values of F_2-layer. Bradley *et al*. (2004) correlated daily changes in f_oF_2 with $M(3000)F_2$ using data collected at the European mid-latitude stations of Slough, Julisruh and Rome over the years 1986–1994. Zhang and Holt (2004) presented correlation between electron density and electron temperature over Millstone Hill for daytime and nighttime periods for different seasons. Zhang *et al*. (2008) presented results from correlative analyses between B_o and h_mF_2, B_o and $M(3000)F_2$, B_1 and $M_{3000}F_2$, B_1 and h_mF_2, and B_1 and B_o using observations recorded at the Asian low-latitude station of Hainan (19.4°N, 109°E), China over the periods from March 2002 to February 2005. The correlation of equatorial vertical drift with ionospheric F_2-layer parameter has not been given serious consideration except those of Obrou *et al*. (2003). The differences between Obrou *et al*. (2003) correlation relationship between h_mF_2 and vertical plasma drift and the current study will be shown later. Using a relatively simple and approximate theoretical model calculation of an upward drift of the equatorial ionospheric plasma, based on the analytic solutions of the continuity equation for daytime solar maximum conditions, Oyekola and Akin Ojo (2008) have examined interrelationship between equatorial ionospheric F_2-region parameters. Again, Oyekola (2011) indicated that drift velocity predicted for Ibadan longitude sector by the latest version of IRI (IRI-2007) could be used to explain the observed daily features of f_oF_2 at the African equatorial site of Ibadan for some selected months during the year 1958 (IGY-era) under sunspot maximum conditions. Furthermore, most of the observed features and behavior of equatorial ionospheric F_2-layer parameters in the African sector and other equatorial stations around the world have been attributed mostly to variations of vertical $V_z = \mathbf{E} \times \mathbf{B}$ plasma drift (e.g., Sambou *et al*., 1998; Radicella and Adeniyi, 1999).

By comparing the behavior of global equatorial F region vertical drift model of Scherliess and Fejer (1999) incorporated in the IRI model (IRI-2007; Bilitza and Reinisch, 2008) with measured and IRI model-predicted F_2-layer parameters, the primary goal of this work is seen as threefold: (1) to describe and quantify the association between vertical drift velocity and F_2-region parameters (using available observational data and IRI model values) at equatorial region. Thus, allows significant insight into the role played by electrodynamics in the equatorial ionosphere; (2) to explore if the diurnal variation of vertical drift could enable us to explain many characteristics features of the diurnal changes in the ionospheric F_2-region characteristics; (3) to examine diurnal and seasonal structures of f_oF_2-h_mF_2 and f_oF_2-$M(3000)F_2$ in order to see if the knowledge of the variation of one can predict the rough variation of the other during low solar flux and magnetic quiet conditions.

2. Observational Data and IRI Model-Predicted Values

In view of the fact that IRI model represents an average ionosphere, we use the monthly hourly median value of f_oF_2 and $M(3000)F_2$ obtained from the ionograms recorded by the ionospheric prediction sounder (IPS42) located at Ouagadougou (12.4°N, 1.5°W; dip latitude 1.5°N) Burkina Faso, in the West African sector during the 1987 solar minimum magnetically quiet periods. The h_mF_2 values were deduced using empirical formula given by Bilitza *et al*. (1979) from the monthly ionosonde parameters, namely f_oF_2, $M(3000)F_2$ and f_oE measured over Ouagadougou station. The standard error in deriving h_mF_2 from the $M(3000)F_2$ factor is estimated to be within about ±(6–9) km over the four seasons.

We used the 2007 version of IRI in this study. IRI outputs were generated for the same geophysical conditions of our ionosonde data using the available model input variables: year, month, day, local time, and the Ouagadougou Observatory geographic coordinates. IRI runs were obtained from IRI website for the equatorial $\mathbf{E} \times \mathbf{B}$ drift velocities (V_z). Table option for thickness parameter (B_o), electron and ion temperatures (T_e, T_i), total electron content (TEC) and electron density (N_e) were obtained from the IRI website. Some

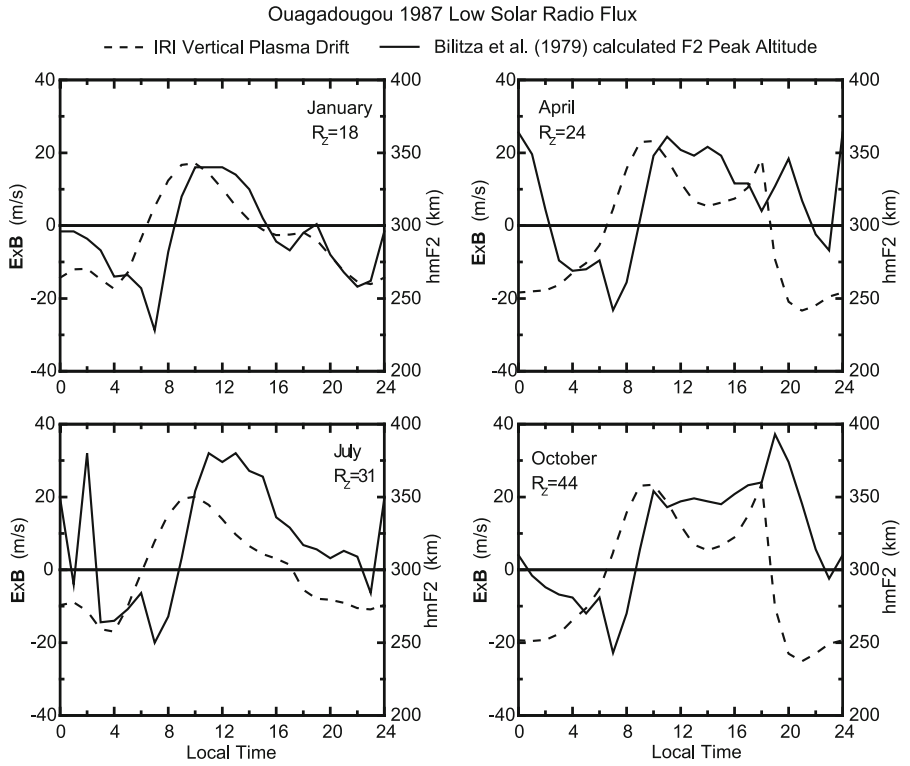

Fig. 1. A comparison between calculated F_2-layer peak altitude (h_mF_2) (right vertical axis, solid curve) and IRI vertical $\mathbf{E} \times \mathbf{B}$ plasma drift velocity (left vertical axis, dashed curve) for January (upper left), April (upper right), July (lower left) and October (lower right) during low solar activity year of 1987. The monthly averaged smoothed sunspot index, R_Z for each month is shown on each panel.

parameters such as plasma density, electron temperature, ion temperature, and total electron content were considered for 300-km altitude. One of the reasons for chosen electron density, in particular, at the height of 300 km is that ionospheric plasma at the F-region (altitude 300 km) is basically a low collision region (Ridley *et al*., 2006). Another reason is that the height centered around 300 km incidentally happens to be transition region from chemically controlled to transport dominated F-region (Oyekola, 2009b and references therein). Hence, it is easy to correlate the effect of vertical drifts with the electron density at a specific height and time.

The data used for this study cover four different seasons: December solstice, March equinox, June solstice and September equinox, represented by January, April, July and October, respectively. These months had average sunspot numbers of 18, 24, 31 and 44, respectively and the yearly-averaged value was about 32. The corresponding geomagnetic A_p index for January, April, July and October was 9, 10, 17 and 21 units, respectively. The annual mean A_p index was approximately 17.

3. Results

This section is presented in the following order: In Subsection 3.1, we examine the relation of IRI representation of the vertical drift identified as Scherliess and Fejer (1999) to ionosonde observed F_2-layer peak data. Local time variation of IRI vertical drift is compared with diurnal changes of IRI F_2-region parameters, predicted for Ouagadougou is our focus in Subsection 3.2. This is followed by a comparison between ionosonde observed F_2-layer critical frequency with peak height F_2-layer and propagation factor (Subsection 3.3).

To aid illustrations, vertical drift and each F_2-layer parameter are merged in one plot and the four seasons are plotted in the same figure as four panels, where the drift velocity is plotted on the left vertical axis (dash curves) and the F_2-layer parameter plotted on the right vertical axis (solid curves) in Figs. 1–8. In each figure the four seasons are put in the following order, January (upper left), April (upper right), July (lower left) and October (lower right).

3.1 Description of equatorial vertical drift and ionosonde F_2-layer peak data

Figure 1 shows typical diurnal and seasonal characteristics behavior of the V_z and h_mF_2 during low solar activity year. As can be seen, January V_z is upward between 0700–1400 LT and completely downward between 1500–0600 LT. The duration of upward drift velocity is relatively shorter. The morning velocity peak occurs at about 1000 LT with a value near 20 m/s, but the evening velocity peak is absent. The drift indicates an earlier downward reversal compared to other seasons. Conversely, the drift in the month of July is positive between 0700 and 1700 LT and negative between 1800–0600 LT. The early morning velocity peak shows up at about 1000 LT with magnitude of ∼20 m/s, while the evening prereversal velocity peak is again absent. April vertical drift is upward between 0700–1800 LT, but mostly downward from 1900 and 0600 LT. Here the daytime drift has largest amplitude at about 0900 LT with typical value of 23 m/s, while the evening prereversal velocity enhancement occurs at dusk with amplitude of about 18 m/s. In contrast, October ver-

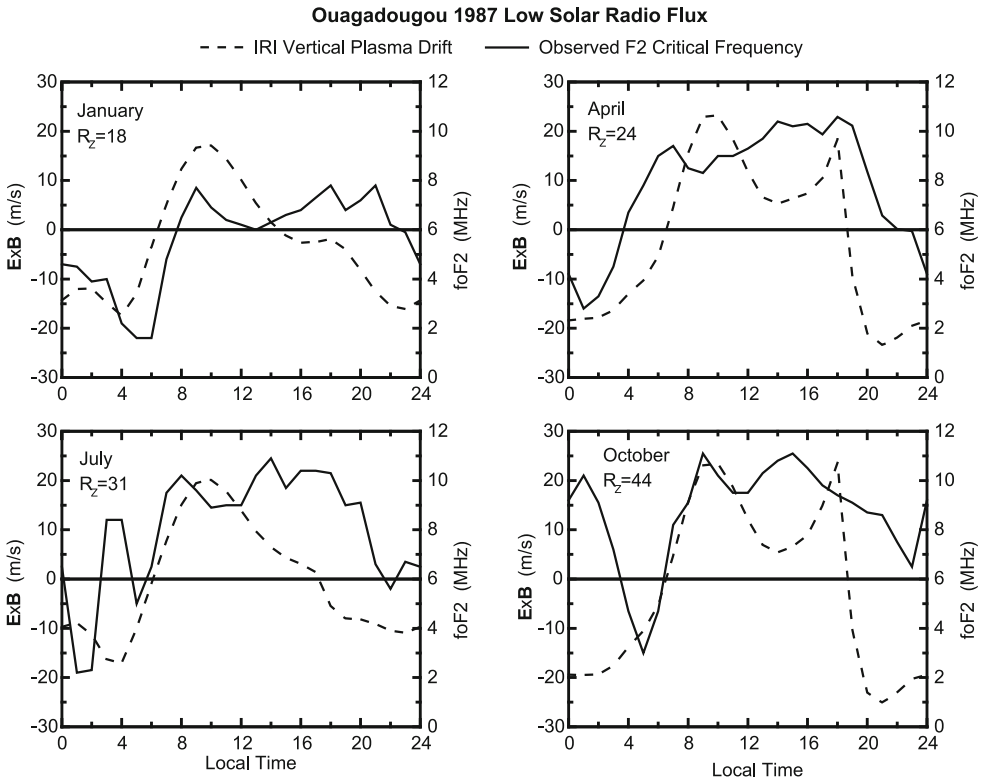

Fig. 2. Same as Fig. 1, but for F_2-layer critical frequency (f_oF_2) and IRI vertical drift.

tical plasma drift solar minimum is mainly upward between 0700 and 1800 local time, but downward from 1900–0600 LT. Here the early morning velocity peak is shifted by an hour later compared to vernal equinox. While occurrence time of the evening prereversal enhancement of the upward drift velocity is the same as that of the month of April, the magnitude of the evening velocity peak is approximately 24 m/s, a full 25% larger than that of April PRE in vertical plasma drift. It is important to state that the general characteristics of IRI model-predicted equatorial vertical drift during low solar flux conditions, emphasize above will be used to contrast the behavior of F_2-layer parameters in Figs. 1–8.

During the months of January and July, h_mF_2 decreases quickly at local afternoon and reaches the lowest value of h_mF_2 at about 2200 LT and 2300 LT for January and July, respectively. While January h_mF_2 decreases rapidly from local midnight with a value of about 296 km and attains early morning (0700 LT) minimum with a value of ∼228 km, July h_mF_2 indicates significant fluctuations between 0000 LT and 0700 LT and shows h_mF_2 minimum of approximately 250 km. After the postsunrise drop, h_mF_2 increases rapidly to attain daytime maximum, which varies from about 340–380 km during 1000–1100 LT for both January and July. January h_mF_2 follows closely the trend in vertical drift during 1000–2200 LT sector. The rate of decrease in the magnitude of plasma drift velocity is faster between about midday and 2200 LT sector during June and July months, which agrees well with variation found in the ionosonde h_mF_2 curves.

In contrast, the morphology of equinoctial h_mF_2 are somewhat similar to each other, except that April h_mF_2 decreases gradually after about local noon till about local sunset and then suddenly rise to attain evening peak in h_mF_2, while h_mF_2 rises fairly linearly within the time interval 0800–1800 LT in October. It can be seen also that both April and October h_mF_2 decreases rapidly from local midnight to reach a minimum value of ∼240 km for April and October at about 0700 LT.

Furthermore, postsunset peak in h_mF_2 occurs between about 1900–2100 LT with typical values of 300–390 km over the four seasons. The evening enhancement in h_mF_2 during solstices periods is considerably smaller than those of equinoxes probably due to absent of PRE in vertical drift during these periods. Except for time shift, the daytime drift peak corresponds to the early morning F_2-layer height peak for all seasons. Equinoctial evening prereversal velocity enhancement also coincides with maximum and minimum in h_mF_2.

Figure 2 compares the diurnal cycle of IRI vertical drift with the local time changes of Ouagadougou ionosonde f_oF_2 for four seasonal periods during solar minimum. Apparently, the local time behavior of vertical drift with f_oF_2 is radically different from each other. Three diurnal peaks of the critical frequency of the F_2-layer are clearly shown. The appearance of forenoon maximum of f_oF_2 occurs at about 0700–0900 LT with typical values of 7.7–11.1 MHz. The postnoon maximum of f_oF_2 ranges from 10.4–11.1 during 1400–1500 LT, except for January f_oF_2 that show up at sunset with a value of about 7.8 MHz. The evening f_oF_2 maximum is within 7.8–10.6 MHz during 1800–2100 LT and is least pronounced in July and October. Analysis of V_z and f_oF_2 curves indicates that the increase in the critical frequency coincides basically with upward direction of drift, and that the decrease corresponds to downward drift. Thus,

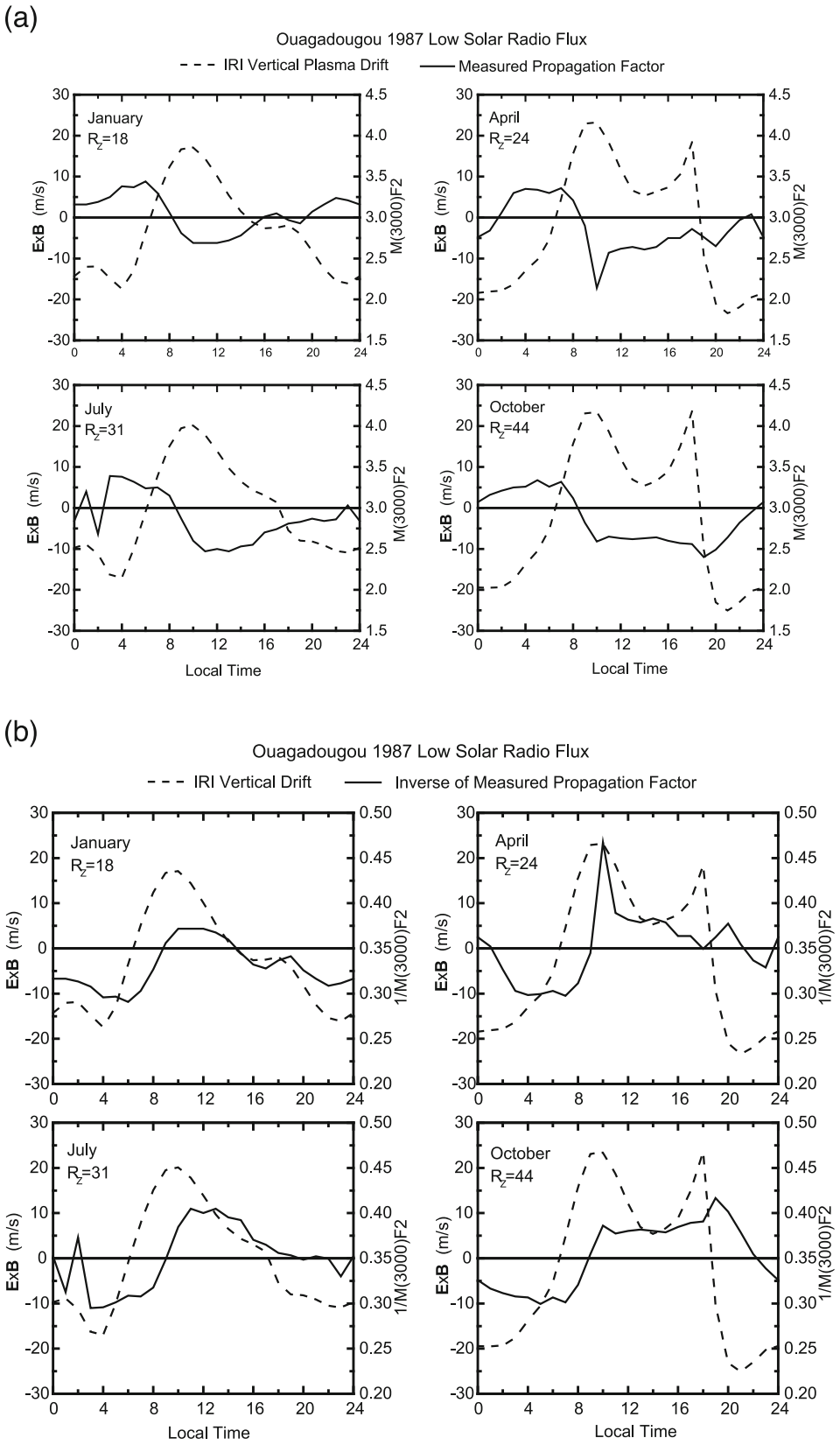

Fig. 3. (a) Same as Fig. 1, but for propagation factor ($M(3000)F_2$) and equatorial vertical plasma drifts. (b) Same as Fig. 1, but for inverse of propagation factor ($1/M(3000)F_2$) and equatorial vertical plasma drifts.

prenoon f_oF_2 peak occurs roughly at the same time as that early velocity peak apart from the month of April in which f_oF_2 maximum and the drift peak are differing by about 3 hours. The evening prereversal enhancement of the upward drift velocity matches the evening f_oF_2 maximum during April. The diurnal variation of f_oF_2 also demonstrates minimum, which ranges from 1.6 to 5.0 MHz at about 0500 LT for all seasons, but not for April and October that show up

Table 1. Correlation coefficient, R, between IRI model equatorial vertical plasma drift and the calculated h_mF_2 and measured f_oF_2 and $M(3000)F_2$ during daytime, nighttime and daytime-nighttime conditions for four different seasons under solar minimum periods of 1987.

Parameters	Month	Day	Night	Day and night
V_z/h_mF_2	January	0.30	0.48	0.60
	April	0.03	−0.41	0.16
	July	0.00	0.22	0.39
	October	0.21	−0.26	0.25
V_z/f_oF_2	January	0.23	0.22	0.45
	April	0.62	−0.48	0.61
	July	−0.29	0.22	0.58
	October	−0.03	−0.25	0.53
$V_z/M(3000)F_2$	January	−0.28	−0.63	−0.75
	April	−0.27	0.54	−0.38
	July	0.01	−0.32	−0.52
	October	−0.22	0.37	−0.36
$V_z/1/M(3000)F_2$	January	0.28	0.66	0.76
	April	0.54	−0.52	0.41
	July	0.56	0.30	0.53
	October	0.54	−0.32	0.35

minimum at about 0100 LT. There is a greater fluctuation of f_oF_2 in July, while a deep trough is seen in October.

The theory predicts that the maximum of the critical frequency should occur at local noon. However, a careful inspection of the f_oF_2 plots, one notes that the f_oF_2 maximum is shifted away from midday by about 3–5 hours, occurring at 0700–0900 local time. So at local noon, depletion of ionization occurs (noon bite-out), although is not well formed in April. Noontime f_oF_2 varies from 6.2 to 9.5 MHz and the corresponding midday value of vertical velocity is in the range of ∼10–14 m/s.

Figure 3(a) displays the diurnal variation patterns between IRI V_z and the measured $M(3000)F_2$ during low solar flux periods for four seasonal conditions. Obviously, the morphological pattern of vertical ionospheric motion and $M(3000)F_2$ is completely different from each month. Going by the plots in Fig. 3(a), one may conclude that there is strong anti-correlation between V_z and $M(3000)F_2$ curves for all seasons. In Fig. 3(b), IRI model-predicted vertical drift for Ouagadougou is plotted with the inverse of observed propagation factor, $1/M(3000)F_2$. The dominant information to come from Fig. 3(b) is that the modeled vertical drift diurnal shape and characteristics appear to match diurnal pattern and features seen in $1/M(3000)F_2$. In particular, the early morning "spike-like" peak of $1/M(3000)F_2$ in April occurs almost the same time as that of morning velocity peak, whereas the evening $1/M(3000)F_2$ maximum is away by about 1–2 hours from PRE of equatorial ionospheric vertical drift.

To quantitatively describe the diurnal variation between the vertical drift model and the measured F_2-layer parameters, we conducted correlation analyses. Table 1 gives the correlation coefficient, R, between plasma drift and observed peak F_2 data when the drift velocity is upward (day) and when the drift is downward (night) and for the entire upward and downward (day and night, all hours). The first tabular column represents correlation relationship between upward drift and the corresponding F_2-layer parameters for the time interval 0700–1400 LT (January), 0700–1800 LT (April), 0700–1700 LT (July) and 0700–1800 LT (October). The second tabular column denotes the correlation factors between downward drift and the corresponding F_2-layer peak data. Here the drift is absolutely in downward direction, from 1500–0600 LT (January), 1900–0600 LT (April), 1800–0600 LT (July) and 1900–0600 LT (October). The third tabular column indicates correlation between combined drift, upward and downward, the whole 24-hour of the day and the corresponding F_2-layer parameters. By carrying out our analysis in this fashion will enable us to quantify the effect of upward drift, downward drift and entire diurnal variation of vertical drift on the ionospheric F_2-layer characteristics. We can see that (1) for daytime conditions, vertical drift and peak height F_2-layer are not related in April and July but exemplify very low positive correlations during January (+0.30) and October (+0.21). Equatorial vertical velocity and F_2-layer critical frequency indicates no correlations in October, extremely low positive correlations in January (+0.23), negatively low correlation in July (−0.29), but good and positive correlation exist in vernal equinox (+0.62). Ionospheric vertical drift and propagation factor demonstrates low anticorrelations relationships, which varies between 0.22–0.28, except in July when there is no link between V_z and $M(3000)F_2$ (∼ +0.01). Association between plasma drift and inverse of $M(3000)F_2$ is dominated by positive correlations, which varies from +0.28 to +0.56, indicating exceptionally low to moderate relationship. (2) For the nighttime conditions, we note that the R values shown in the second tabular column is drastically higher than those values found for the daytime conditions. Here V_z-h_mF_2 shows very low positive and negative correlations in July (+0.22) and October (−0.26), but exhibits moderate positive and negative corre-

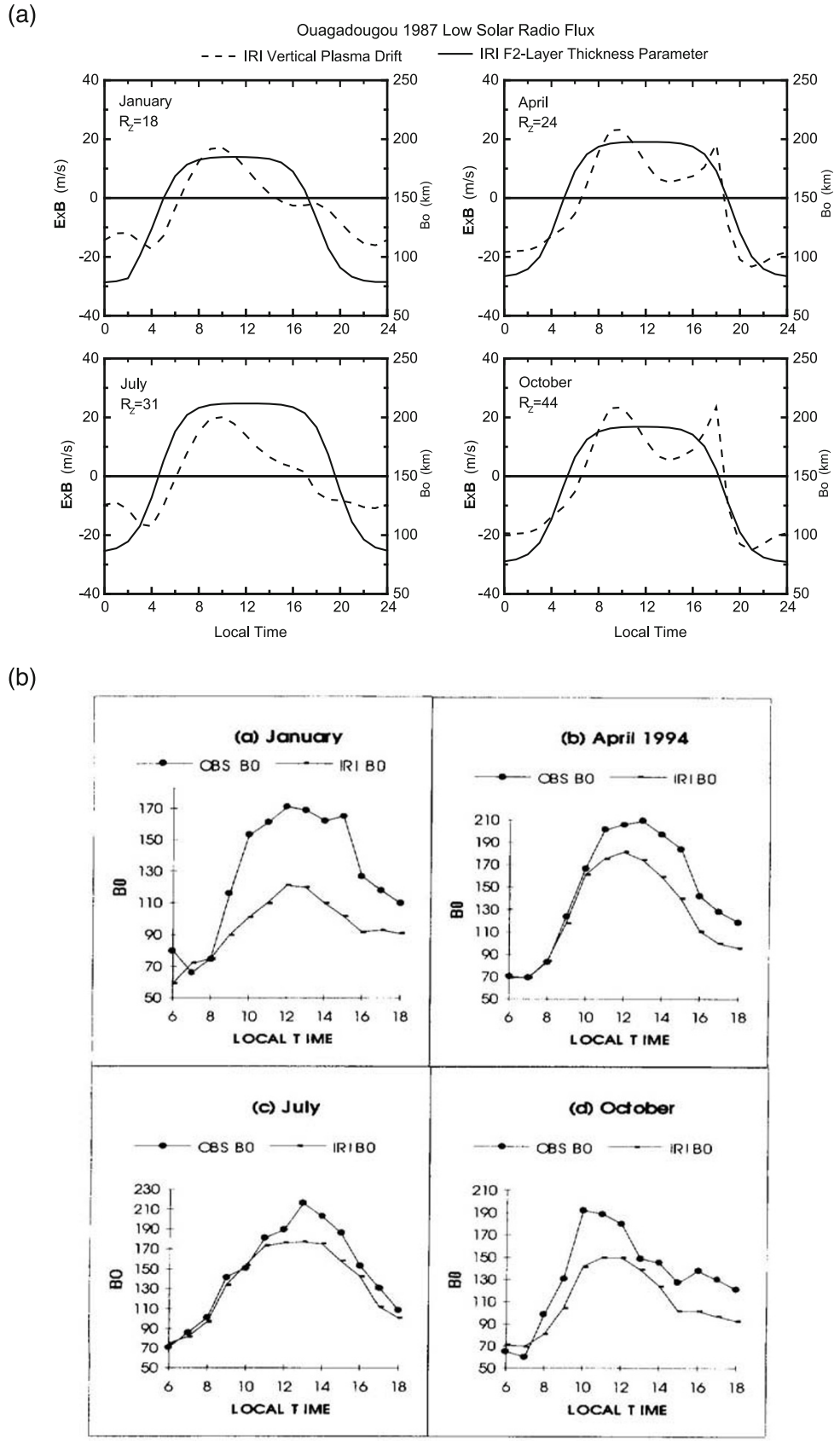

Fig. 4. (a) A comparison between IRI F_2-layer thickness parameter (B_o) (right vertical axis, solid curve) and IRI equatorial vertical plasma drift velocity (left vertical axis, dashed curve) for January (upper left), April (upper right), July (lower left) and October (lower right) during low solar minimum conditions. (b) Daytime F_2-layer thickness parameter (B_o) measured at Ouagadougou during January (left top), April (right top), July (bottom left) and October (bottom right) for solar minimum conditions of 1994. (c) Same as Fig. 4(b), but for average measured F_2-layer bottomside thickness parameter. (Reprinted from *J. Atmos. Sol.-Terr. Phys.*, **60**(3), Adeniyi, J. O. and S. M. Radicella, Diurnal variation of ionospheric profile parameters B_0 and B_1 for an equatorial station at low solar activity, 381–385, doi:10.1016/S1364-6826(97)00118-1, Copyright 1998, with permission from Elsevier.)

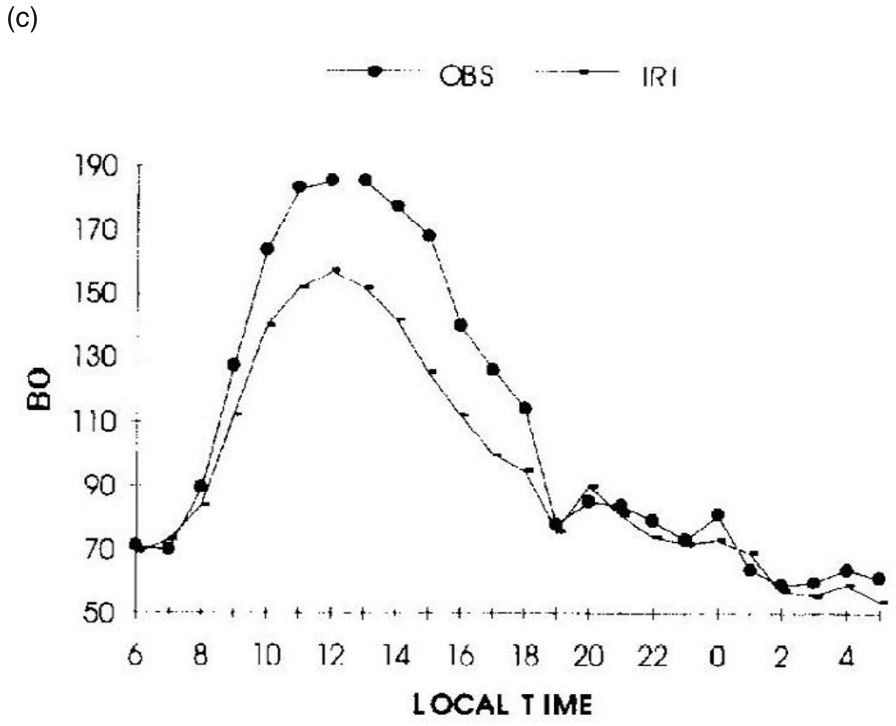

Fig. 4. (continued).

lations in January (+0.48) and April (−0.41). V_z-f_oF_2 indicates very small connection during January (+0.22), July (0.22) and October (−0.25), whereas the drift is negatively and moderately related to F_2-layer critical frequency in April (~ -0.48). V_z-$M(3000)F_2$ had low positive and negative correlations (<0.40), but moderately positive (+0.54) and good negative correlations (−0.63) exist in April and January, respectively. On the other hand, V_z-$1/M(3000)F_2$ is positively well-linked in January, positively low correlation exist in July, but negative correlations are found in equinoxes with low value in October and moderate value in April. It is interesting to note that the correlation relationship between V_z-h_mF_2 is opposite that of V_z-$M(3000)F_2$ for both daytime and nighttime conditions in each season, confirming the strong anticorrelations between h_mF_2 and $M(3000)F_2$. (3) When the drift is both upward and downward, the entire diurnal changes, the correlations are predominantly positive except for V_z-$M(3000)F_2$ association, which completely demonstrates inverse correlations for all seasons. R ranges from 0.16–0.60 (positive), 0.45–0.61 (positive), 0.36–0.75 (negative) and 0.35–0.76 (positive) for equatorial vertical drift and h_mF_2, f_oF_2, $M(3000)F_2$ and $1/M(3000)F_2$, respectively. In general, since the values of R are from extremely low to good correlations with barely statistically significant value of R exists, the preliminary conclusion is that equatorial vertical drift plays less significant role in the variations of the measured F_2-layer parameters. This need further study.

3.2 Analysis of equatorial plasma drift and the IRI-simulated F_2-layer parameters

In this subsection we analyze the link between IRI equatorial vertical plasma drift and other IRI model predictions of F_2-layer parameters. Figure 4 shows the trends in the modeled vertical $\mathbf{E} \times \mathbf{B}$ drift velocity and the simulated F_2-layer bottomside thickness parameter for four different seasons. The figure demonstrates typical characteristics of diurnal cycle and seasonal cycle during low solar flux conditions. As can be seen the daytime B_o-T_{ab} curve from 0700–1600 LT remain practically constant at a value of approximately 200 km for all seasons, but shows significant variation at other times (1700–0600 LT). The modeled thickness parameter follows the behavior of the vertical drift from 0400–0800 LT during solstices, but from 0400–0800 LT and 1600–2000 LT during equinoxes. Since it is difficult to get bottomside thickness parameter derived from the experimental data for Ouagadougou station of precisely the same year. We looked for year with similar solar and geophysical conditions. Figure 4(b) depicts the daytime morphology of B_o for Ouagadougou and IRI-90 model-prediction during low solar activity year of 1994 for four seasons. Coincidentally these months correspond to the months/seasons that we analyzed in this work. The average sunspot number for that period was 30 and the corresponding geomagnetic A_p index was about 16. Figure 4(c) presents average diurnal variation of inferred and modeled B_o parameter over Ouagadougou. Figures 4(a) and 4(b) were adopted from the work of Adeniyi and Radicella (1998). Naturally, the observed equatorial B_o present similar structure for all seasons, symmetrical about midday during solstices, but the noontime peak is shifted away by 1–2 hours in equinoxes. The nighttime behavior (Fig. 4(c)) indicates somewhat "wave-like" pattern parallel to longitudinal behavior presented by Liu *et al.* (2010) and seasonal variations of B_o reported by Chen *et al.* (2006) and Zhang *et al.* (2008). Comparisons between Figs. 4(a), (b) and (c) hints that daytime B_o should correspond to daytime upward ver-

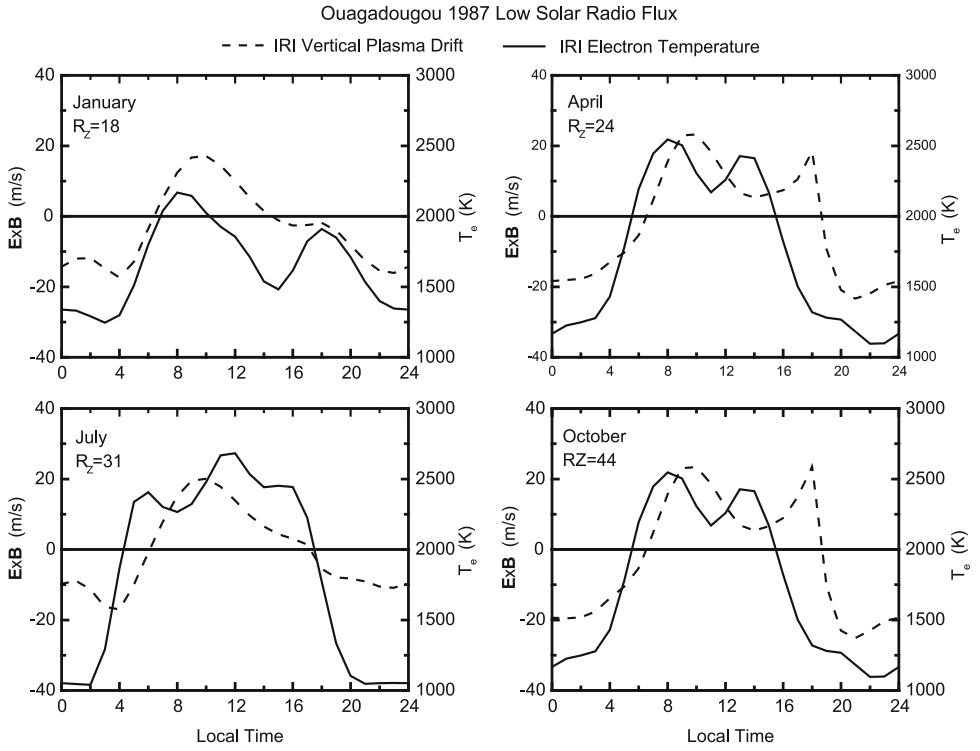

Fig. 5. Same as Fig. 4, but for IRI electron temperature (T_e) and IRI equatorial vertical drift.

tical drift, particularly during the solstices. Nonetheless, the result must be regarded with caution until B_o inferred from the experimental observations and quantified the correlation between the equatorial vertical drift and F_2-layer bottomside thickness. Hence, further analysis is necessary.

The variation of simulated equatorial ionospheric drift and IRI electron temperature for quiet magnetic activity and low solar flux conditions is depicted in Fig. 5. Visually, Fig. 5 shows that there is strong positive correlation between ionization temperature and electrodynamic $\mathbf{E} \times \mathbf{B}$ drift velocity for all seasons, but not for July. The electron temperature indicates steep rise in the early morning reaches a peak (morning overshoot) at about 0800 LT (January, April, and October). Afterward decrease with a minimum around 1500 LT (January), at 1100 LT in equinoctial months. A second peak (evening overshoot) occurs after midday just before sunset around 1400 LT in April and October but show up around dusk hour in January. One other important feature found in Fig. 5 is that morning peak in T_e occurs ~1 hour earlier than the morning maximum seen in vertical plasma drift in January and equinoctial months. Generally the morning overshoot is slightly higher than the evening overshoot, except for July, where the two peaks are approximately comparable. Additionally, July electron temperature shows a midday peak that is higher than the morning and evening temperature peaks.

The diurnal variations of IRI vertical drift and IRI model-predicted ion temperature are shown in Fig. 6, respectively, for January, April, July, and October. As can be seen, the changes in ionospheric drift velocities seem not to have link with the variations observe in ion temperature in comparison to the electron temperatures (Fig. 5). It should be noted that the diurnal variation of ion temperature presents fairly "wave-like" patterns in April and October.

Figure 7 displays diurnal morphological structures of modeled drift velocity and IRI total electron content during low solar flux equinoxes and solstitial periods. The total electron content is measured in TECU (1 TECU = 10^{16} el/m^2). The regular characteristic features of the diurnal variation of IRI model-predicted TEC are as follows: The pre-sunrise minimum, which occurs at about 0400 LT for the four seasons and almost coincides with the period when vertical drift reaches predawn minimum. The morning enhancement in TEC varies between about 7–12 TECU and occurs during 0800–0900 LT. There is afternoon and early evening TEC peak, which has a magnitude ranging from 8–10 TECU between about 1500–1700 LT. The morning TEC peak appears to correspond to the daytime drift velocity peak in all seasons, implying likely linkage. The TEC peak also indicates larger equinoctial morning value compared to those of solstice seasons. On the other hand, morning and afternoon TEC enhancement in April are somewhat similar. October morning peak is about 17% higher than the postnoon peak in TEC. There is also a deep midday trough (noon bite-out) seen in all seasons, which has a magnitude varying from about 5 to 8 TECU. Generally the overall variation patterns of vertical drift and ionospheric total electron content are quite impressive.

Figure 8 gives the diurnal changes in electron density for January, April, July and October. We can see that IRI model simulated electron density displays a diurnal cycle low at around 0400 LT, except for the month of April, which indicates minima at about 0300 LT and another at 0600 LT. Morning electron density peak occurs during 0800–0900 LT with characteristic value of 0.6–0.8 $\times$ 10^{12} el/m^3 and afternoon and evening peak appears around 1500–1700 LT,

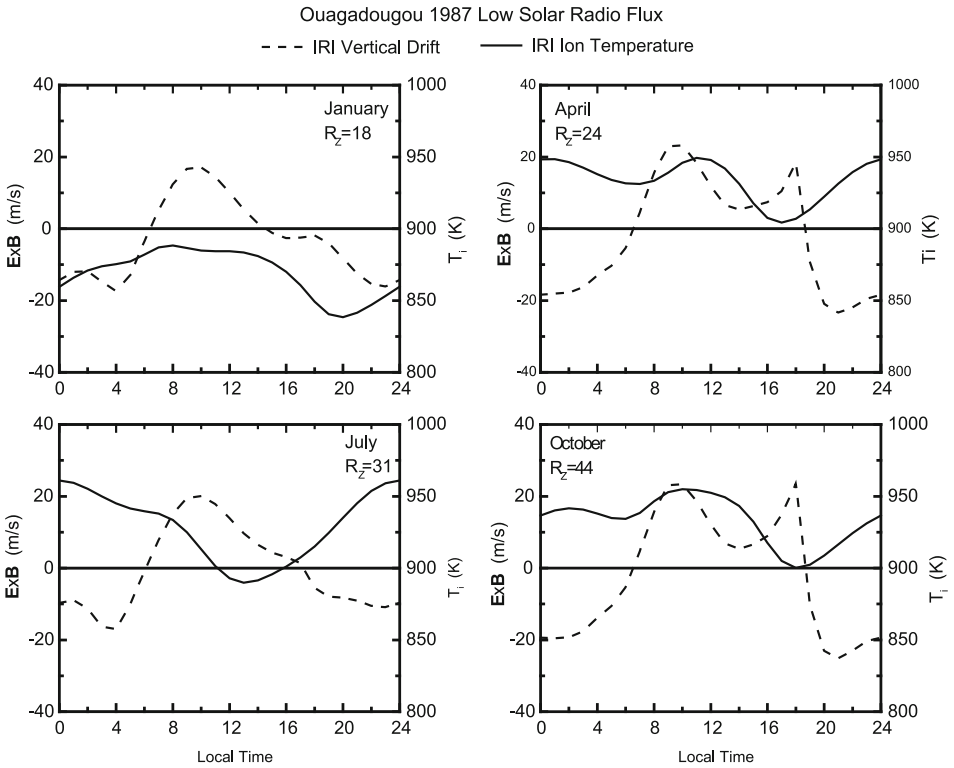

Fig. 6. Same as Fig. 4, but for IRI ion temperature (T_i) and IRI vertical plasma drift.

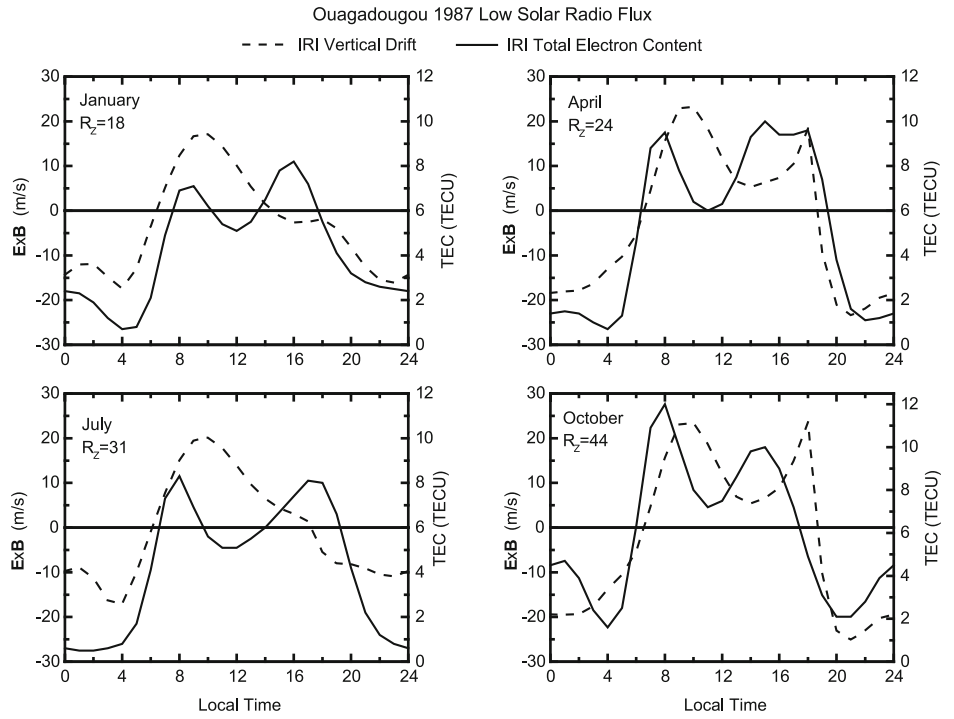

Fig. 7. Same as Fig. 4, but for IRI total electron content (TEC) and IRI vertical drift.

but has magnitude varying between approximately 0.8–1.2×10^{12} el/m^3 over the four seasons. In January presunrise N_e peak is noticed with a value near 0.7×10^{12} el/m^3. Notice that the diurnal cycle low is most pronounced in October. There is also a noontime minimum for all seasons, which varies from about 0.5–0.8 $\times$ 10^{12} el/m^3. It is quite interesting to see that during vernal equinox, the evening velocity peak and the evening electron density enhancement occurs virtually at around 1800 LT. Immediately after the peak is reached, the modeled electron density follows the behavior of the IRI vertical drift.

Table 2 summarizes the correlation analysis results between equatorial vertical plasma drift and the most essential IRI model-predicted F_2-layer parameters presented in

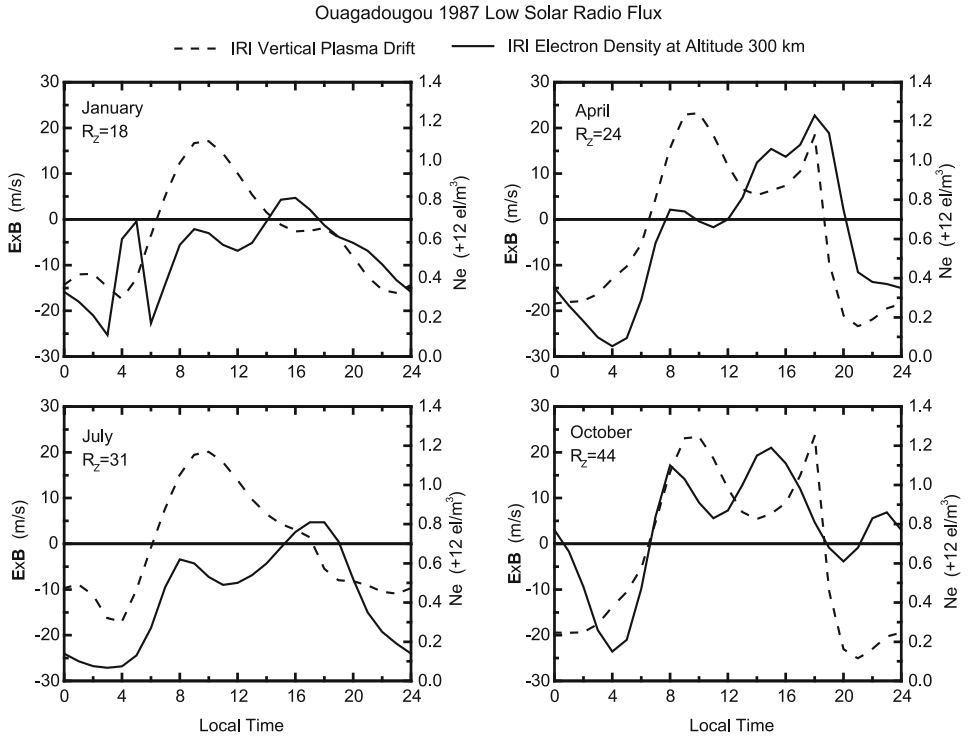

Fig. 8. Same as Fig. 4, but for IRI electron density (N_e) and IRI vertical drift.

Table 2. Correlation coefficient, R, between IRI model equatorial vertical drift and IRI-B_o, IRI-T_e, IRI-T_i, IRI-TEC, and IRI-N_e at 300 km height during daytime, nighttime and daytime-nighttime conditions for four different seasons under low solar flux periods of 1987.

Parameters	Month	Day	Night	Day and night
V_z/B_o	January	0.45	0.71	0.83
	April	−0.07	0.85	0.91
	July	0.47	0.55	0.82
	October	−0.30	0.88	0.90
V_z/T_e	January	0.73	0.81	0.87
	April	−0.04	0.82	0.77
	July	0.31	0.31	0.78
	October	−0.27	0.83	0.74
V_z/T_i	January	0.49	0.01	0.61
	April	0.31	−0.35	−0.20
	July	0.30	−0.41	−0.68
	October	−0.01	0.12	0.24
V_z/TEC	January	0.34	0.81	0.75
	April	−0.46	0.51	0.82
	July	−0.43	0.62	0.70
	October	−0.46	0.37	0.77
V_z/N_e	January	0.21	0.49	0.38
	April	−0.10	0.00	0.62
	July	−0.88	0.54	0.59
	October	−0.86	−0.51	0.59

Figs. 4(a)–8. As in Table 1, the first, second and third tabular column represents value of R when the drift is positive (day), negative (night) and both positive and negative (day and night), respectively. During the daylight hours, V_z-B_o relationship indicates low to moderate correlation, but is not related in April. V_z-T_e indicates no association again in the month of April, low correlation is seen in July and October, but highly positively correlated is observed in the month of January. V_z-T_i demonstrates low correlations in April and July, no link in October, but moderate positive correlation exists in January. V_z-TEC correlation relationship exhibits reasonable inverse correlations except for January,

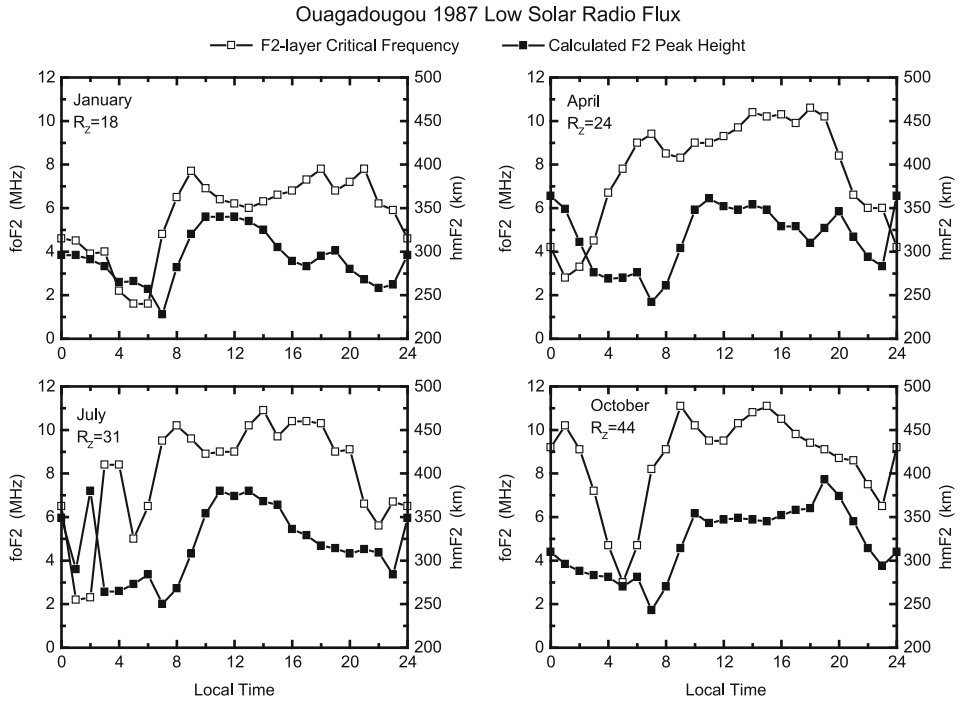

Fig. 9. A comparison between measured monthly median F_2-layer critical frequency (f_oF_2) (left vertical axis) and estimated monthly median peak height F_2-layer at Ouagadougou during January (top left), April (top right), July (bottom left) and October (bottom right) for solar minimum year of 1987.

which shows low positive correlations. V_z-N_e is strongly anti-correlated in July and October, but indicates poor relationship in January and April. Overall, a full 15% of the correlation coefficients are statistically significant, signifying that electrodynamic $\mathbf{E} \times \mathbf{B}$ drift contributes little to daytime variations of F_2-layer parameters. In contrast, during the nighttime ionosphere, vertical drift and F_2-layer parameters are better correlated than the dayside ionosphere. The correlation coefficient ranges from 0.55–0.88, 0.31–0.83, 0.01–0.41, 0.37–0.81 and 0.00–0.54, respectively for V_z-IRI B_o, V_z-T_e, V_z-T_i, V_z-TEC and V_z-N_e. On average, a full 35% of the correlation coefficients are statistically significant. The relationship between vertical drift and F_2-layer characteristics improve greatly when the both positive and negative drift values are correlated with F_2-layer parameters. Here, the association is dominated by positive correlations with 60% of the correlation factor being statistically significant, 25% are well correlated, 5% indicates low correlation and 10% show poor relationship. On the basis of this analysis, we conclude, in general, that equatorial electrodynamics play a major role in the variation of ionospheric F_2 characteristics.

3.3 Comparisons among ionosonde measured F_2-layer peak parameters

We further examine the relationship between measured f_oF_2 with h_mF_2 and $M(3000)F_2$. Figure 9 contrasts the f_oF_2 diurnal variations for January, April, July and October. The essential features of f_oF_2 and h_mF_2 have rigorously addressed earlier in this paper (see observations 1 and 2). The main results in Fig. 9 is that while the prominent f_oF_2 diurnal cycle low occurs at around 0500 LT for all seasons, except for the month of April which indicates postmidnight minimum, h_mF_2 signifies diurnal cycle low at about two hours later for all seasons. In contrast, the early morning peak in f_oF_2 appears between about 0700–0900 LT for all seasons, but morning peak in h_mF_2 occurs at about 2–3 hour away from the occurrence time of morning f_oF_2 peak. The diurnal and seasonal fluctuations patterns during solstice periods are exceptionally different and as well different from those of equinoxes, which are largely dissimilar.

Figure 10 gives a comparison of the local time changes in F_2-layer critical frequency and corresponding changes in propagation factor during magnetically quiet and low solar flux conditions for the four seasons. The plots demonstrate considerable opposite variations between the two parameters.

Table 3 presents correlation coefficients which show the differences in the relationship between f_oF_2-h_mF_2 and f_oF_2-$M(3000)F_2$ during daytime (0600–1800 LT), nighttime (1900–0500 LT), and daytime-nighttime. At daytime, f_oF_2-h_mF_2 is positively correlated with correlation factor ranges from low to moderate correlations. In contrast, during the night poor correlation relationship exists in January and April, low and negative correlation in July, but moderate and positive correlations in October. The overall daytime correlations results are not encouraging; the correlation factor is within 0.12–0.56 and entirely positive. On the other hand, f_oF_2-$M(3000)F_2$ correlation values predominantly illustrate inverse relationship for daytime, nighttime, and daytime-nighttime. At daytime, abnormally low correlations exist in April, low value of R in July, well correlated in January and October. At nighttime correlation relationship is much smaller in April and July, moderate in October, well connected and statistically acceptable in January. On average, still low in April and July, highly correlated,

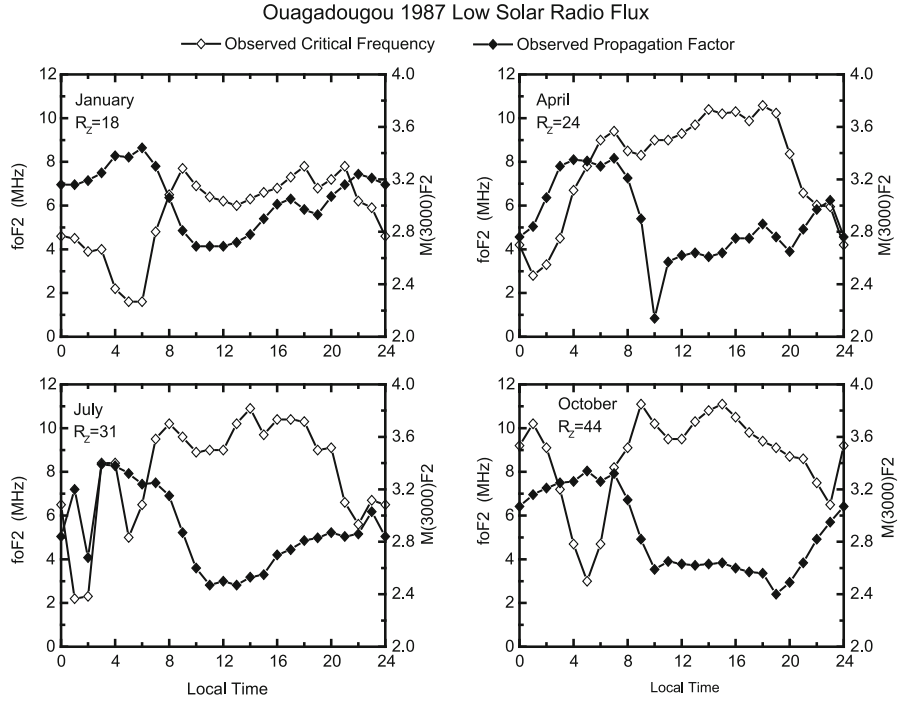

Fig. 10. Same as Fig. 9, but for the observed f_oF_2 and measured propagation factor ($M(3000)F_2$).

Table 3. Correlation coefficient, R, between measured f_oF_2 and inferred h_mF_2, and measured f_oF_2 and $M(3000)F_2$ at Ouagadougou during quiet-day and low solar flux periods of 1987 for daytime, nighttime and daytime-nighttime conditions for four different seasons.

Parameters	Month	Day	Night	Day and night
f_oF_2/h_mF_2	January	0.48	0.07	0.41
	April	0.35	−0.15	0.12
	July	0.20	−0.39	0.13
	October	0.58	0.52	0.56
$f_oF_2/M(3000)F_2$	January	−0.65	−0.76	−0.68
	April	−0.23	−0.13	−0.32
	July	−0.36	0.14	−0.33
	October	−0.72	−0.46	−0.63

but not significant correlation values are obtained in January and October.

4. Discussion

This paper deals with the correlation of the equatorial electrodynamic plasma ($\mathbf{E} \times \mathbf{B}$) drifts derived from IRI model with a set of important F_2-layer ionospheric/upper thermospheric parameters for some chosen months during quiet-day low solar flux periods, in order to determine the electrodynamic dependent of ionospheric characteristics at F-layer heights and to what degree vertical drift component can explain a number of regular characteristic features of the diurnal and seasonal variations of these parameters.

It is of note that the former authors, Obrou *et al.* (2003) used ionosonde data recorded at Korhogo, Cote-d'Ivoire (9.3°N, 5.4°W, dip latitude: 2°S) in West-African region to investigate ways of improving the representation of equatorial F_2 peak height, h_mF_2 in the IRI. The authors correlated observed h_mF_2 at Korhogo with the equatorial F region vertical drift given by the model of Scherliess and Fejer (1999) during low solar activity year of 1995. The monthly averaged sunspot number, R_{z12} was 18 and corresponding geomagnetic A_p index was 12. The current research utilizes F_2 peak height, h_mF_2 inferred from ionosonde $M(3000)F_2$ measurements from the Ouagadougou Observatory (12°N, 1.5°W; dip: 1.5°N) in West-African sector to study the link between calculated h_mF_2 and the IRI/Scherliess and Fejer (1999) global equatorial vertical drift model during low solar flux year of 1987. The monthly averaged smoothed sunspot number was about 32 and the yearly-averaged geomagnetic A_p index for that period was approximately 17. The behaviors of estimated equatorial h_mF_2 and empirical plasma drift are correlated; hence the effects of vertical drift on h_mF_2 are investigated. Detailed comparisons between the two stations unveil the following points: First, the behavior of observed h_mF_2 and IRI vertical drift at Korhogo during solstice periods is completely opposite to those seen between calculated h_mF_2 and IRI vertical drift at Ouagadougou. Specifically, between about 1500 and 2300 LT in January 1995 at Korhogo, the variation of h_mF_2 and V_z is comparable to the trend noticed in h_mF_2 and V_z between 1100 and 2300 local time in 1987 in the month of July at

Ouagadougou. While that of July 1995 at Korhogo from local time between 0100–2300 LT corresponds to that of January 1987 at Ouagadougou between 1100–2300 LT. This reverse relationship is also evident in equinoctial months (April and October). In addition, the prominent equinoctial feature of equatorial ionosphere, postsunset peak in h_mF_2 is clearly evident at Ouagadougou, indicating consistent observations of the F_2 layer uplifting even at lower solar flux periods. This feature is absolutely absent at Korhogo probably due much smaller value of sunspot index during 1995 compared to that of 1987. Second, at Korhogo, the authors found no clear correlation between measured h_mF_2 and modeled vertical drift by day, but strong positive correlation by night. At Ouagadougou, the daytime correlation relationship between calculated h_mF_2 and IRI plasma drift is dramatically low and no correlations exist during the daytime. At night, the derived h_mF_2 is weakly anti-correlated with V_z in equinoctial months (April and October). For daynight, correlation is still low but not for January where V_z-h_mF_2 are well connected. Third, the remarkable disparities found at the two sites within West-African sector, Korhogo and Ouagadougou may probably due to the differences in geomagnetic latitudes. This means that drastically opposite behaviors seen at Korhogo and Ouagadougou reveals some differences that are probably consistent with their magnetic northern hemisphere and southern hemisphere locations. In addition, the differences of our results from Obrou *et al.* (2003) may partly come from the longitudinal structure of h_mF_2. The observations given above are in accord with the findings reported by Bilitza *et al.* (2004b) using data collected at the two stations, Korhogo and Ouagadougou during low, moderate and high solar activity years of 1995 and 1985, 1998 and 1993, and 2000 and 1991, respectively; to examine variability of f_oF_2 at the two stations. In a comparative analysis between f_oF_2 observations and IRI model at low latitude station, Ibadan, Nigeria (7.4°N, 3.9°E; 5°S dip angle), Oyekola (2011) found IRI model to be larger than the measured f_oF_2 in June from 1900–0500 LT and September from 1900–2300 LT. In contrast, Bittencourt and Chryssafidis (1994) using data from a low latitude station, Fortaleza, Brazil (3.9°S, 38.45°W, dip angle: 11.5°S) under comparable solar and geophysical conditions analyzed by us, reported that the observed F_2 peak electron density (or f_oF_2) were generally higher than those predicted by the IRI model in the same months of June and September. The reason for such difference may lie in the fact that the geomagnetic peculiarity of the Brazilian equatorial region characterized by its magnetic declination with weaker magnetic field intensity (Abdu *et al.*, 2010). The f_oF_2 (or N_mF_2) and h_mF_2 measurements in Ibadan and Fortaleza indicates that opposite effects are seen in F_2 peak parameters as one moves away from magnetic equator and moves toward anomaly peak implying anomaly peak effects in one hand. On the other hand, confirmed the anomalous and difficult behavior of F_2-region to predict (Brum *et al.*, 2011).

It is observed that the variation of h_mF_2 in Fig. 1 is very similar to f_oF_2 diurnal variation in Fig. 2 shown also in Fig. 9, where minimum of f_oF_2 is observed at midnight except for April. In addition, the behavior of both h_mF_2 and f_oF_2 differs from typical opposite diurnal variation at mid-latitudes where f_oF_2 peak occurs around noon but h_mF_2 peaks by midnight. This unexpected opposite behavior in ionospheric F_2 layer peak parameters at equatorial and mid-latitudes is essentially latitude difference, which seems to be connected to the geomagnetic field configuration. Both f_oF_2 (N_mF_2) and h_mF_2 have peculiarities in the equatorial zone. It is well known that the daytime upward plasma drift velocity lifts electrons to higher altitudes in the equatorial region, where recombination loss rate is low. In addition, the fact that the source of electron production is still present during the daytime that will favor the daytime higher values of h_mF_2 and enhanced f_oF_2 (or N_mF_2) at low solar activity. At nighttime, the converse is the case. The reversal of the vertical drift to the downward direction occurs shortly after the postsunset increase. Thus in the postsunset ionosphere, downward drift pushes electrons to lower heights in the equatorial region, where chemical recombination rate is high, coupled with the fact that photoionization of atomic oxygen by solar UV radiation ceases. What is then observed is lowering of the peak height from postsunset to sunrise sector with reduced plasma density. A close look at Fig. 2, one would therefore expect a greater nighttime downward plasma drift toward the equator in October than in April. This explains why f_oF_2 minimum occurs at midnight in April and not in October. A more reliable experimental comparison of plasma drifts and F_2 layer peak parameters at near equatorial region is needed to confirm this conclusion.

Generally the time variations of equatorial ionospheric F_2-layer parameters are dominated by several characteristic features such as, diurnal low (depression), morning peak (prenoon peak), midday trough (noon bite-out), postnoon peak and evening enhancements. These observed features and many others were hitherto explained on the basis of equatorial plasma dynamics associated with the Appleton ionization anomaly (EIA—Equatorial Ionization Anomaly).

The correlation relationship between IRI vertical plasma drift and the F_2-layer characteristics are typically low, but there is a significant correlation, R exceeding 0.70, 0.80 and 0.90, typically between V_z and B_o, V_z and T_e, together with V_z and TEC during the daytime-nighttime (upward and downward drift). There are fewer instances during daylight and nighttime hours where statistically significant correlations are also observed. Inverse correlation prevails for V_z and measured propagation factors relationship, except for the nighttime in April and October, which shows low positive correlation values. It is worth noting that correlation analysis results for vertical drift and derived h_mF_2 are totally opposite those of V_z and measured $M(3000)F_2$, whereas vertical drift and $1/M(3000)F_2$ correlation results is fully consistent with the association between V_z and h_mF_2. These results validate the strong anti-correlations between h_mF_2 and $M(3000)F_2$, for empirical relationship between h_mF_2 and $M(3000)F_2$, see Bilitza *et al.* (1979). It is also worthwhile to point out that while daytime correlation relationship indicates positive value, the nighttime correlation factor, R, present opposite effect in most circumstances. In other words, if daytime correlation is negative, the nighttime correlation may be positive (see

Tables 1 and 2).

Due to rather straightforward approach of correlating equatorial electrodynamics with ionospheric F_2-layer characteristics, quantifying the correlations between the F_2-layer parameters and vertical drift in one hand, and among the F_2-layer peak parameters on the other hand, is still a complex and challenging issue, yet we cannot completely rule out the likelihood of other influences on the variation of the ionosphere/thermosphere parameters.

A reasonable explanation of the behavior highlighted above can be sought in the following speculation. During magnetically quiet daytime at the magnetic equator, the polarization electric field of E-layer dynamo origin is pointing eastwards. It is mapped into the F-layer by the magnetic lines of force. In the F-region, the $E \times B$ drift controls the plasma transport across the magnetic field. Charge particles are lifted by $\mathbf{E} \times \mathbf{B} = V_z$ drift velocity, which generally revert downward during the night. Quiet daytime drift carries the plasma at altitudes up to 700 km above the F_2 peak (at 300 to 450 km altitudes). The plasma is then displaced by ambipolar diffusion along magnetic lines of force under gravity and plasma pressure gradients (e.g., Sambou *et al*., 1998, and references therein). Ionization tends to move along magnetic field lines, giving rise to the well known "equatorial fountain effect" that originates in the so-called equatorial anomaly of the geomagnetic low-latitude ionosphere. The latitude profiles of F_2 peak electron density remain smooth at daytime hours with a minimum centered at the dip equator, in the general appearance of a "trough". In local time this trough is modulated along a noon bite-out shape due to stronger upward drift velocity at midday hours. Consequently, fountain effect mechanism explains in part the observed midday minimum of F_2-layer critical frequency (equivalently peak F_2 density) (Observation 2), total electron content (Observation 7) and electron concentration (Observation 8). Moreover, the enhancement in the vertical drift of the F-layer plasma at sunset is indicative of a sudden removal of plasma from the equatorial ionosphere. The net effect is a rise in peak height F_2-layer and concurrent sharp drop in electron density immediately after sunset.

The important interesting features found in the diurnal behavior of the F_2-layer can also be explained basically by the interplay between effects of ionization production by solar ultraviolet radiation, loss through charge exchange and transport by diffusion, electrodynamic drift and neutral wind processes that occurs in the upper ionosphere. A regular feature in the equatorial ionosphere, morning enhancements observed virtually in all F_2-layer parameters is probably due to persistent photoelectron heating (e.g., Zhang *et al*., 1999). Thermospheric neutral winds have also been recognized to be an important candidate responsible in part to the nighttime behavior of equatorial ionosphere (e.g., Villa *et al*., 1998).

Moreover, recent investigations have indicated that direct dynamic forcing, changes in temperature and thermospheric composition and daily changes in E-region dynamo electric fields that produce drifts in the F-region are other factors affecting the electron density in the F_2-layer (Mendillo *et al*., 2002). Zhang and Holt (2004) pointed out that thermospheric temperature could have fundamental effects on the ionospheric electron density by changing the neutral composition and winds and by altering the production and diffusion chemical loss equilibrium of the ionospheric ions. It has been reported that the upper ionosphere is greatly influenced by magnetospheric processes from above and lower atmospheric processes from below even during geomagnetic quiet conditions. Physical sources of ionospheric variability are studied in detail by Forbes *et al*. (2000) and by Rishbeth and Mendillo (2001). Several former investigations proposed that tides and planetary waves play an important role in the electrodynamic of lower thermosphere which, in turn cause significant variations in the equatorial vertical plasma drifts; for analysis of the propagation mechanism and effects of atmospheric tides and planetary waves, see recent publications by Zou *et al*. (2000), Muller-Wodarg *et al*. (2001), Lastovicka (2006), Pancheva *et al*. (2006), Kil *et al*. (2007), Lin *et al*. (2007).

5. Conclusions

We have analyzed ionosonde measurements made at near-equatorial dip latitude, Ouagadougou, Burkina Faso, for four months representing equinoxes and solstices during low level of solar activity and some set of appropriate parameters provided by the latest version of IRI (IRI-2007) model to study in detail how the quiet-day IRI equatorial vertical drift can be used to explain diurnal structure as well as various significant regular features of F_2-layer characteristics. Quantitative analyses between vertical drift and F_2-layer parameters are also examined. On the basis of our analysis, the major highlights and the main conclusions of our investigation are summarized as follows:

1. The average diurnal and season-to-season patterns between the time variation of equatorial vertical drift and local time changes of F_2-layer parameters are generally satisfactory; implying that the main features found in diurnal variations of F_2-layer parameters may be attributed to electrodynamic conditions in the equatorial ionosphere. The relationship between vertical drift and F_2-layer parameters is largely seasonally dependent.
2. IRI model vertical plasma drift is in a good correlation with IRI-B_o, IRI-T_e and IRI-TEC, whereas little or no acceptable correlation is obtained with observational evidence.
3. The daytime (upward drift), nighttime (downward drift) and daytime-nighttime (upward and downward drift) correlations relationship provides some evidence that equatorial ionosphere is largely influenced by other mechanisms controlling at day/night or combined effect of electrodynamic drift plus other mechanisms. The results illustrate complicated behavior of the ionosphere, also.
4. Statistically significant correlation coefficient that exists between equatorial vertical drift velocity and electron temperature hints that upper ionosphere and upper thermosphere are strongly coupled.
5. The current research shed more light on the importance of equatorial ionospheric electrodynamics through the plasma fountain effect. Nonetheless, the work essen-

tially recapitulates the success of the IRI simulation in explaining observed ionospheric and other phenomena. Finally, these findings do not necessary apply to latitude regimes outside the West African region.

Acknowledgments. The author acknowledges benevolence of the United State National Oceanic and Atmospheric Administration (NOAA) for providing equatorial F_2-layer parameters from the IRI website at: http://omniweb.gsfc.nasa.gov/vitmo/iri_vitmo.html. The author wish to acknowledge the support of Dr. Rudi Hanbaba, Centre National d'Etudes des Telecommunications, Lannion, France, for providing observational data used in this work. The author is also indebted to three anonymous referees who gave worthwhile evaluation and critical remarks on the draft of this paper. Their comments and suggestions rigorously helped in improving the scientific value of this research paper. Thanks are also due to the guest editor, Dr. Dieter Bilitza, for his impressive and encouraging remarks in carrying out the revised version of this work.

References

Abdu, M. A., I. S. Batista, C. G. M. Brum, J. W. MacDougall, A. M. Santos, J. R. de Souza, and J. H. A. Sobral, Solar flux effects on the equatorial evening vertical drift and meridional winds over Brazil: A comparison between observational data and the IRI model and the HWM representations, *Adv. Space Res.*, **46**, 1078–1085, 2010.

Adeniyi, J. O. and S. M. Radicella, Diurnal variation of ionospheric profile parameters B_0 and B_1 for an equatorial station at low solar activity, *J. Atmos. Sol.-Terr. Phys.*, **60**(3), 381–385, doi:10.1016/S1364-6826(97)00118-1, 1998.

Alken, P., A quiet time empirical model of equatorial vertical plasma drift in the Peruvian sector based on 150 km echoes, *J. Geophys. Res.*, **114**, A02308, doi:10.1029/2008JA013751, 2009.

Bilitza, D., The International Reference Ionosphere 1990, National Space Science Data Center, NSSDC/WDC-A-R&S Reports 90-22, Greenbelt, Maryland, 1990.

Bilitza, D., International Reference Ionosphere 2000, *Radio Sci.*, **36**(2), 261–275, 2001.

Bilitza, D., International Reference Ionosphere 2000: Examples of improvements and new features, *Adv. Space Res.*, **31**(3), 757–767, 2003.

Bilitza, D. and B. W. Reinisch, International Reference Ionosphere 2007: improvements and new parameters, *Adv. Space Res.*, **42**(4), 599–609, doi:10.1016/j.asr.2007.07.048, 2008.

Bilitza, D., N. M. Sheikh, and R. Eyfrig, A global model for the height of the F2-peak using M3000 values from the CCIR numerical maps, *Telecomun. J.*, **46**(9), 549–553, 1979.

Bilitza, D., K. Rawer, and B. W. Reinisch (eds.), Path toward improved ionosphere specification and forecast models, *Adv. Space Res.*, **33**(6), 988–992, 2004a.

Bilitza, D., O. K. Obrou, J. O. Adeniyi, and O. Oladipo, Variability of foF2 in the equatorial ionosphere, *Adv. Space Res.*, **34**, 1901–1906, 2004b.

Bittencourt, J. A. and M. Chryssafidis, On the IRI model predictions for low latitude ionosphere, *J. Atmos. Terr. Phys.*, **56**(8), 995–1009, 1994.

Bradley, P. A., S. S. Kouris, I. Stanislawska, D. N. Fotiadis, and G. Juchnilowski, Day-to-day variability of the IRI electron density height profile, *Adv. Space Res.*, **34**, 1869–1877, 2004.

Brum, C. G. M., F. S. Rodrigues, P. T. dos Santos, A. C. Matta, N. Aponte, S. A. Gonzalez, and E. Robles, A modeling study of foF2 and hmF2 parameters measured by the Arecibo incoherent scatter radar and comparison with IRI model predictions for solar cycles 21, 22, and 23, *J. Geophys. Res.*, **116**, A03324, doi:10.1029/2010JA015727, 2011.

Chen, H., L. Liu, W. Wan, B. Ning, and J. Lei, A comparative study of the bottomside profile parameters over Wuhan with IRI-2001 for 1999–2004, *Earth Planets Space*, **58**, 601–605, 2006.

Fejer, B. G., The electrodynamics of the low-latitude ionosphere: recent results and future challenges, *J. Atmos. Terr. Phys.*, **59**(13), 1465–1482, 1997.

Fejer, B. G., D. T. Farley, R. F. Woodman, and C. Calderon, Dependence of equatorial F-region vertical drifts on season and solar cycle, *J. Geophys. Res.*, **84**, 5792–5796, 1979.

Fejer, B. G., E. R. de Paula, S. A. Gonzales, and R. F. Woodman, Average vertical and zonal F-region plasma drifts over Jicamarca. *J. Geophys. Res.*, **96**, 13901–13906, 1991.

Forbes, J. M., S. E. Palo, and X. Zhang, Variability of the ionosphere, *J. Atmos. Sol. Terr. Phys.*, **62**, 685–693, 2000.

Heelis, R. A., Electrodynamics in the low and middle latitude ionosphere: A tutorial, *J. Atmos. Terr. Phys.*, **66**, 825–838, 2004.

Kelley, M. C., *The Earth's Ionosphere: Plasma Physics and Electrodynamic*, pp. 65–154, Academic Press, San Diego, Calif., U.S.A., 1989.

Kil, H., S.-J. Oh, M. C. Kelley, L. J. Paxton, S. L. England, E. Talaat, K.-W. Min, and S.-Y. Su, Longitudinal structure of the vertical $\mathbf{E} \times \mathbf{B}$ drift and ion density seen from ROCSAT-1, *Geophys. Res. Lett.*, **34**, L14110, doi:10.1029/2007GL030018, 2007.

Lastovicka, J., Forcing of the ionosphere by waves from below, *J. Atmos. Sol. Terr. Phys.*, **68**, 479–497, 2006.

Lin, C. H., W. Wang, M. E. Hagan, C. C. Hsiao, T. J. Immel, L. M. Hsu, J. Y. Liu, L. J. Paxton, T. W. Fang, and C. H. Liu, Plausible effect of atmospheric tides on the equatorial ionosphere observed by the FORMOSAT-3/COSMIC: Three-dimentional electron density structures, *Geophys. Res. Lett.*, **34**, L11112, doi:10.1029/2007GL02965, 2007.

Liu, L., W. Wan, B. Ning, M.-L. Zhang, M. He, and X. Yue, Longitudinal behaviors of the IRI-B parameters of the equatorial electron density profiles retrieved from FORMOSAT-3/COSMIC radio occultation measurements, *Adv. Space Res.*, **46**, 1064–1069, 2010.

Mendillo, M., H. Rishbeth, R. G. Roble, and J. Wroten, Modelling F2-layer seasonal trends and day-to-day variability driven by coupling with the lower atmosphere, *J. Atmos. Terr. Phys.*, **64**, 1911–1931, 2002.

Muller-Wodarg, I. C. F., A. D. Aylward, and T. J. Fuller-Rowell, Tidal oscillations in the thermosphere: a theoretical investigation of their sources, *J. Atmos. Terr. Phys.*, **63**(9), 899–914, 2001.

Obrou, O. K., D. Bilitza, J. O. Adeniyi, and S. M. Radicella, Equatorial F2-layer peak height and correlation with vertical ion drift and M(3000)F2, *Adv. Space Res.*, **31**(3), 513–520, 2003.

Oyekola, O. S., A study of evolution/suppression parameters of equatorial postsunset plasma instability, *Ann. Geophys.*, **27**, 1–5, 2009a.

Oyekola, O. S., Equatorial F-region vertical ion drifts during quiet solar maximum, *Adv. Space Res.*, **43**, 1950–1956, 2009b.

Oyekola, O. S., Comparisons of foF2 with IRI model and equatorial vertical drifts, *Adv. Space Res.*, **48**(8), 1318–1326, doi:10.1016/j.asr.2011.06.027, 2011.

Oyekola, O. S. and Akin-Ojo, Effect of vertical plasma transport on ionospheric $F2$ region parameters at equatorial latitude, *Adv. Space Res.*, **41**(9), 1500–1509, doi:1010.1016/jasr.2007.11.017, 2008.

Oyekola, O. S. and L. B. Kolawole, Equatorial vertical $\mathbf{E} \times \mathbf{B}$ drift velocities inferred from ionosonde measurements over Ouagadougou and the IRI-2007 vertical ion drift model, *Adv. Space. Res.*, **46**, 604–612, doi:10.1016/j.asr.2010.04.003, 2010.

Oyekola, O. S. and C. O. Oluwafemi, Morphology of F-region vertical $\mathbf{E} \times \mathbf{B}$ drifts in the African sector using ionosonde measurements, *Ann. Geophys.*, **50**(5), 615–625, 2007.

Oyekola, O. S. and C. O. Oluwafemi, Solar and geomagnetic trends of equatorial evening and nighttime F-region vertical ion drifts, *J. Geophys. Res.*, **113**, A12318, doi:10.1029/2008JA013315, 2008.

Oyekola, O. S., Akin-Ojo, J. Akinrimisi, and E. R. dePaula, Seasonal and solar cycle variability in F-region vertical plasma drifts over Ouagadougou, *J. Geophys. Res.*, **112**, A12306, doi:10.1029/2007JA012560, 2007.

Oyekola, O. S., Akin-Ojo, and J. Akinrimisi, A comparison of ground and satellite observations of F-region vertical velocity near the dip equator, *Radio Sci.*, **43**, RS1005, doi:10.1029/2007RS003699, 2008.

Pancheva, D. V. *et al.*, Two-day wave coupling of the low-latitude atmosphere–ionosphere system, *J. Geophys. Res.*, **111**, A07313, doi:10.1029/2005JA011562, 2006.

Radicella, S. M. and J. O. Adeniyi, Equatorial ionospheric electron density below the F2 peak, *Radio Sci.*, **34**, 1153–1163, 1999.

Ridley, A. J., Y. Deng, and G. Toth, The global ionosphere-thermosphere model, *J. Atmos. Sol. Terr. Phys.*, **68**, 839–864, 2006.

Rishbeth, H. and M. Mendillo, Patterns of F2 layer variability, *J. Atmos. Sol. Terr. Phys.*, **63**, 1661–1680, 2001.

Rush, C. M. and A. D. Richmond, The relationship between the structure of equatorial anomaly and the strength of the equatorial electrojet, *J. Atmos. Terr. Phys.*, **35**, 1171–1180, 1973.

Sambou, E., P. M. Vila, and A. T. Kobea, Non-trough foF2 enhancements at near-equatorial dip latitudes, *Ann. Geophys.*, **16**, 711–720, 1998.

Scherliess, L. and B. G. Fejer, Radar and satellite global equatorial F region vertical drift model, *J. Geophys. Res.*, **104**(A4), 6829–6842, 1999.

Sultan, P., Linear theory and modeling of the Rayleigh-Taylor instability leading to the occurrence of equatorial spread F, *J. Geophys. Res.*, **101**, 26875–26891, 1996.

Villa, P., D. Rees, P. Merrien, and E. Kone, Fabry-Perot interferometer measurements of neutral winds and F2-layer variations at the magnetic equator, *Ann. Geophys.*, **16**, 731–737, 1998.

Zhang, M.-L., W. Wan, L. Liu, and J. K. Shi, Variability of the behavior of the bottomside (Bo, B1) parameters obtained from the ground-based ionograms at China's low latitude station, *J. Adv. Space*, **42**, 695–702, 2008.

Zhang, S.-R. and J. M. Holt, Ionospheric plasma temperature during 1976-2001 over Millstone Hill, *J. Adv. Space*, **33**, 963–969, 2004.

Zhang, S.-R., S. Fukao, W. L. Oliver, and Y. Otsuka, The height of the maximum ionospheric electron density over the MU radar, *J. Atmos. Terr. Phys.*, **61**, 1367–1383, 1999.

Zou, L., H. Rishbeth, I. C. F. Muller-Wodarg, A. D. Aylward, G. H. Millward, T. J. Fuller-Rowell, D. W. Idenden, and R. J. Moffett, Annual and semiannual variations in the ionospheric F2-layer. I. Modelling, *Ann. Geophys.*, **18**, 927–944, 2000.

O. S. Oyekola (e-mail: oyedemio@yahoo.com)